



Research paper

# Water-soluble inorganic photocatalyst for overall water splitting

Yu Hang Li<sup>a</sup>, Yun Wang<sup>b</sup>, Li Rong Zheng<sup>c</sup>, Hui Jun Zhao<sup>b</sup>, Hua Gui Yang<sup>a,\*</sup>,  
Chunzhong Li<sup>a,\*</sup>



<sup>a</sup> Key Laboratory for Ultrafine Materials of Ministry of Education, School of Materials Science and Engineering, East China University of Science and Technology, 130 Meilong Road, Shanghai 200237, China

<sup>b</sup> Centre for Clean Environment and Energy, Gold Coast Campus, Griffith University, Queensland 4222, Australia

<sup>c</sup> Beijing Synchrotron Radiation Facility, Institute of High Energy Physics, Chinese Academy of Sciences, Beijing 100049, China

## ARTICLE INFO

### Article history:

Received 17 November 2016

Received in revised form 21 February 2017

Accepted 1 March 2017

Available online 1 March 2017

### Keywords:

Overall water splitting

Photocatalysts

Sodium molybdate salt

Water-soluble inorganics

## ABSTRACT

In the past 45 years, the search for semiconductors as active photocatalysts for overall water splitting has focused on insoluble materials and their hybrids. An important question is whether soluble semiconductors have the capacity for photocatalysis or similar applications. The dissolved semiconductors will lose the energy band structures for light absorption; however, the undissolved part in saturated solution can still generate electrons and holes under illumination. Unfortunately, this possibility has never been realized. Here we clearly demonstrate the use of a water-soluble sodium molybdate salt as an effective photocatalyst. The material can photocatalyze simultaneously the oxidation and reduction of water under band-gap irradiation. We anticipate that, as a large and traditional class of chemical compounds, the soluble semiconductors may have great potential to be applied in numerous important applications such as catalysis, photovoltaics, light emitting diodes and artificial photosynthesis.

© 2017 Elsevier B.V. All rights reserved.

## 1. Introduction

The search for suitable photocatalysts for splitting of water into hydrogen (H<sub>2</sub>) product is one of the noble missions of material science [1]. One of the critical challenges that must be overcome to enable the practical use in environmental and clean energy areas is finding efficient and stable photocatalysts for overall water splitting (OWS) without sacrificial agents [2,3]. During the past forty years, overwhelming attention has focused on insoluble inorganics (e.g. TiO<sub>2</sub>, ZnO and BiVO<sub>4</sub>), [4–8] insoluble organics (e.g. g-C<sub>3</sub>N<sub>4</sub> or other polymers), [9–11] soluble organics (e.g. molecular photocatalysts) [12] and their hybrids as photocatalysts [13–16]. Unfortunately, none of currently reported photocatalysts can be utilized for large-scale applications of H<sub>2</sub> generation [17]. Thus, it is of great importance to expand potential candidates for water splitting field. The soluble inorganics can be dissolved in water, which arises because of the attraction between positive and negative charges, resulting in the decomposition of crystalline structures and thus losing energy band structures for light absorption. Noteworthy, more solute added in its saturated solution will remain as crystals, and these undissolved ionic compounds would retain the

geometrical structures for absorbing light and transferring photogenerated carriers. These suggest that the undissolved soluble inorganic semiconductors may represent a new class of photocatalysts for OWS. However, the possible application of soluble inorganic semiconductors as photocatalysts has never been fulfilled, to the best of our knowledge.

Herein, we find a typical soluble inorganic semiconductor, sodium molybdate salt (Na<sub>2</sub>MoO<sub>4</sub>), as an effective photocatalyst for overall water splitting under band-gap irradiation after precipitating in its saturated solution (see Fig. 1 for schematic mechanism). Experimentally observed results clearly demonstrate the OWS capacity of undissolved Na<sub>2</sub>MoO<sub>4</sub> as photocatalyst, recording an apparent quantum yield of 0.36% at 365 nm; whereas the dissolved Na<sub>2</sub>MoO<sub>4</sub> solution exhibits no activity. In addition, we present that the undissolved photocatalyst is very stable for OWS for more than two weeks. The findings in this work constitute the first experimental evidence of the capacity of soluble inorganics for photocatalytic OWS, and may hold the promise for the development of soluble inorganics as catalysts for artificial photosynthesis and other scalable technologies that harness solar energy and convert it to fuel.

\* Corresponding authors.

E-mail addresses: [hgyang@ecust.edu.cn](mailto:hgyang@ecust.edu.cn) (H.G. Yang), [czli@ecust.edu.cn](mailto:czli@ecust.edu.cn) (C. Li).

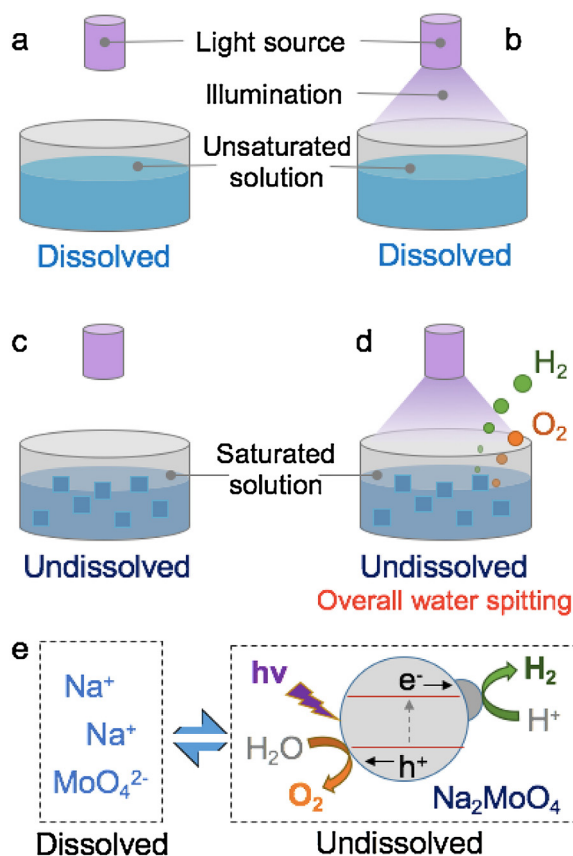


**Fig. 1.** Plausible reaction mechanism of the undissolved  $\text{Na}_2\text{MoO}_4$  as photocatalyst for overall water splitting. No photocatalytic activity of water splitting can be detected in unsaturated solution in darkness (a) or under illumination (b), because of the missing energy band structures of the dissolved  $\text{Na}_2\text{MoO}_4$  sample and the transparency of the solution. No hydrogen or oxygen evolved on undissolved  $\text{Na}_2\text{MoO}_4$  photocatalyst when the light source was masked (c), whereas stoichiometric  $\text{H}_2$  and  $\text{O}_2$  evolved on undissolved  $\text{Na}_2\text{MoO}_4$  photocatalyst under illumination (d). (e) The undissolved ionic compounds would retain the geometrical structures for absorbing light and transferring photogenerated carriers for overall water splitting.

## 2. Experimental methods

### 2.1. Synthesis of photocatalyst

In the preparation of the photocatalyst, a two-step synthesis process was involved. Firstly, 1.06 g of commercial  $\text{Na}_2\text{CO}_3$  (Sinopharm) and 1.44 g of  $\text{MoO}_3$  (Sinopharm) was carefully ground, which was carried out in a ball mill with wet grinding method (ethanol, 24 h under rotation speed of 300 r.p.m.). Then we prepared the thermally treated sample through annealing ground mixture in a Muffle furnace at  $700^\circ\text{C}$  for 600 min. The resulting powder can be collected after the furnace cooling down to room temperature. The  $\text{Rh}_{2-x}\text{Cr}_x\text{O}_3$  cocatalyst was loaded by an impregnation method. The as-prepared  $\text{Na}_2\text{MoO}_4$  sample was mixed with an appropriate amount of  $\text{RhCl}_3$  and  $\text{Cr}(\text{NO}_3)_3$  ethanol solution. Then the suspension was stirred at  $80^\circ\text{C}$  until the liquid was evaporated. After being dried, the mixture was heated in a Muffle furnace at  $300^\circ\text{C}$  for 2 h, and  $\text{Rh}_{2-x}\text{Cr}_x\text{O}_3/\text{Na}_2\text{MoO}_4$  photocatalyst can be collected after the furnace cooling down to room temperature.

### 2.2. Materials characterizations

The crystal structure was determined using X-ray diffraction (D/MAX 2550 VB/PC). The structure of the catalysts was examined by SEM (S-3400N) and TEM (TECNAI F-30, 300 kV). Brunauer-

Emmett-Teller (BET) surface area measurements were performed at 77 K on a Micromeritics ASAS 2460 adsorption analyzer in  $\text{N}_2$ -adsorption mode. The loading amount of the cocatalyst was tested by ICP-atomic emission spectroscopy (Varian 710 ES). Further, the chemical states of the elements in catalysts were studied by XPS (ESCALAB 250Xi), and the binding energy of the C 1s peak at 284.9 eV was taken as an internal reference. Mo K-edge absorption spectra and in-situ analysis were performed on the 1W1B beamline of the Beijing Synchrotron Radiation Facility (BSRF), China, operated at  $\sim 200$  mA and  $\sim 2.5$  GeV. Standard  $\text{Na}_2\text{MoO}_4$  powder was used as reference sample. A UV torch (365 nm, average intensity of irradiation is about  $3.5 \text{ mW cm}^{-2}$ ) was used in in-situ XAFS analysis to illuminate the unsaturated  $\text{Na}_2\text{MoO}_4$  solution that in a sealed vessel during the XAFS spectra collection. All samples were measured in the transmission mode.

### 2.3. Photocatalytic tests

The photocatalytic water splitting tests were carried out in a glass closed-gas-circulation system with a top-irradiation-type reaction vessel (LabSolar  $\text{H}_2$ ). The temperature of the reactant solution was maintained at  $20^\circ\text{C}$  by a flow of cooling water during the tests. A quantity of 1.05 g of photocatalyst that dissolved and precipitated in 10 ml of pure water was added into the reaction vessel for the water splitting test under the illumination of a 365 nm LED. The reactants were sonicated for 10 min for better dispersion and then purged with argon for 5 min to expel the dissolved oxygen. The amounts of evolved hydrogen and oxygen were monitored by an online gas chromatograph (GC-2014C) equipped with a thermal conductivity detector (TCD) and a methanizer and a flame ionization detector (FID) with argon as carrier gas. No air should have remained in the system after evacuation by a vacuum pump. The apparent quantum efficiency (AQE) was measured under the above photocatalytic reaction conditions. It was determined that the average intensity of irradiation was  $5.2 \text{ mW cm}^{-2}$  and the irradiation area was  $12.56 \text{ cm}^2$ . The AQE was calculated according to the following equation (see details in Supporting Information):

$$\text{AQE} = (\text{number of reacted electrons}) / (\text{number of incident photons}) \times 100\%$$

$$= (\text{number of evolved } \text{H}_2 \text{ molecules} \times 2) / (\text{number of incident photons}) \times 100\%.$$

### 2.4. Theoretical calculations

All density functional theory (DFT) computations were performed using the Vienna *ab initio* simulation package (VASP) based on the projector augmented wave (PAW) method [18,19]. Electron-ion interactions were described using standard PAW potentials, with valence configurations of  $4s^2 4p^6 5s^2 4d^4$  for Mo,  $2s^2 2p^6 2s^1$  for Na, and  $2s^2 2p^4$  for O. A plane-wave basis set was employed to expand the smooth part of wave functions with a cut-off kinetic energy of 520 eV. For the electron–electron exchange and correlation interactions, the functional parameterized by Perdew–Burke–Ernzerhof (PBE) [20], a form of the general gradient approximation (GGA), was used throughout. The  $\text{Na}_2\text{MoO}_4$  crystal was modelled with the primary unit cell including 4 Na atoms, 2 Mo atoms and 8 O atoms. The theoretical lattice constant is  $9.290 \text{ \AA}$ , which is ca. 2% larger than the experimental value. Before the analysis of the electronic properties, the geometry was optimized. All the atoms were allowed to relax until the Hellmann–Feynman forces were smaller than  $0.001 \text{ eV/\AA}$ . The convergence criterion for the electronic self-consistent loop was set to  $10^{-5} \text{ eV}$ . We performed Brillouin-zone integrations using a gamma-centred ( $4 \times 4 \times 4$ ) k-point grid for the structural optimization. And a denser

Download English Version:

<https://daneshyari.com/en/article/6454167>

Download Persian Version:

<https://daneshyari.com/article/6454167>

[Daneshyari.com](https://daneshyari.com)